Functionalized COFs with Quaternary Phosphonium Salt for Versatilely Catalyzing Chemical Transformations of CO_2

WANG Tianxiong[1,2#], MU Zhenjie[1#], DING Xuesong[1✉] and HAN Baohang[1,2✉]

Currently, it encounters great challenges to accomplish catalyzing various kinds of carbon dioxide(CO_2) conversion reactions efficiently with single catalyst, let alone control the interplay among catalytic efficiency and selectivity evenly. Here, we prepared a functional covalent organic framework, [PTPP]$_{X\%}$-TD-COF[PTPP=3-bromopropyltriphenylphosphonium; TD=1,3,5-tri(4-aminophenyl)benzene-1,4-diformylbenzene], by immobilizing the quaternary phosphonium salt onto the skeleton of COFs through a post-synthesis strategy for versatilely catalyzing reduction of CO_2 and CO_2 fixation on epoxide and aziridine facilely. With the typical features of COFs(such as porosity and ordered structure) and catalytic activity of the quaternary phosphonium salt, [PTPP]$_{X\%}$-TD-COF possesses an intensely synergistic effect for catalyzing the chemical transformations of CO_2. Noteworthily, the quaternary phosphonium salt functionalized COFs catalyze the CO_2 reduction reaction with amine and phenylsilane to produce formylated and methylated products under gentle reaction conditions with high selectivity and efficiency. Furthermore, [PTPP]$_{X\%}$-TD-COF shows high catalytic ability in CO_2 chemical fixation reactions.

Keywords Covalent organic framework; Quaternary phosphonium salt; Heterogeneous catalysis; Carbon dioxide; Chemical transformation

1 Introduction

Excessive atmospheric concentration of carbon dioxide would lead to dramatic climate change[1—4], which is adverse to biological survival. However, the toughest problem is that, the climate risks would persist for millennia if we totally rely on natural carbon cycles to reduce the concentration of CO_2 even though we halt human carbon emission immediately[5,6]. Therefore, it's necessary to take anthropogenic actions to control the atmospheric content of CO_2 for diminishing the long-term threat from climate changes. Everything has its two-sidedness. CO_2 is one kind of nontoxic, abundant, and renewable carbon resource[7], which can be taken as raw material to synthesize high-value industrial products[8—12]. However, CO_2 has not yet been extensively applied in industrial production since its inherent thermodynamic and kinetic limitations, which are ascribed to the highest oxidation state carbon atom in CO_2[13—15]. Thus, it's indispensable to develop efficacious catalysts for performing a series of CO_2 chemical conversions under mild conditions. Indeed, multiple chemical transformation reactions have been researched in the last decades, such as the CO_2 reduction reaction to prepare formate, formic acid, methanol[16], formamide[17,18], methylamine[19], or carbon monoxide[20], and CO_2 fixation reaction to produce cyclic carbonate[21—23] or 5-aryl-2-oxazolidinone[24,25]. Recently, various catalysts, such as metal-based catalysts[26,27] and organic catalysts[18] were developed for catalyzing CO_2 chemical transformations. Nevertheless, these catalysts always have some drawbacks more or less, for instance, the metal-based catalysts are prone to be deactivated and the organic catalysts are usually unstable. Furthermore, there are plenty of common shortcomings in recyclability, efficiency, selectivity, etc. Therefore, it's necessary to develop superior metal-free, heterogeneous catalysts for resolving these issues.

Recently, various ionic liquids have been widely applied in carbon conversion[28—30]. Among them, the most ionic liquids are nitrogen-based derivatives, which are commonly used to catalyze carbon fixation reactions with epoxide. As another element in the same main group(VA) as nitrogen, phosphorus-based catalysts are rarely studied. Although quaternary phosphonium salt/P(III) species is typical Lewis base, phosphonium cation has ability to accept the electron[31]. Furthermore, it would be beneficial to performing as catalytially active site when considering the atom diameters of phosphorus and nitrogen. Because the bigger atom size always means that the nucleus has a weaker constraining force to the outside valence electrons. Resembling the transition metals, phosphorus atom participates in nucleophilic or electrophilic reaction with little hindrance to change the shape of electron cloud and accept/donate electrons[32,33]. Therefore, quaternary phosphonium salt is one kind of more versatile nucleophilic reagents than quaternary ammonium salt in organic synthesis[34,35]. Although the CO_2 adduct of P-ylide has been

✉ HAN Baohang
hanbh@nanoctr.cn
✉ DING Xuesong
dingxs@nanoctr.cn
# These authors contributed equally to this work.
1. CAS Key Laboratory of Nanosystem and Hierarchical Fabrication, CAS Center for Excellence in Nanoscience, National Center for Nanoscience and Technology, Beijing 100190, P. R. China;
2. University of Chinese Academy of Sciences, Beijing 100049, P. R. China

synthesized by Matthews and co-workers in 1966[36], quaternary phosphonium salt as catalyst has not shown enough applications in CO_2 conversion. The first example using phosphonium salt as homogenous catalyst to catalyze CO_2 transformation was reported by Lu and co-workers in 2015[21]. However, it's not so ideal for homogenous catalysts under efficient and applicative reaction conditions. The reason why phosphonium-based ionic liquid does not achieve the expected result may be elaborately hypothesized that there is no single catalytic system that can independently adjust the interplay among activity, selectivity, and efficiency[37]. Considering that the homogenous catalyst is strenuous to recycle and the scope of application with high efficiency has some restrictions, the novel phosphorus-based catalysts with high activity, selectivity, efficiency, stability, and recyclability need further research and development. Porous organic polymers(POPs) are preferred supports for molecular catalysts owing to their high porosity and stability. The POPs with phosphonium salt on the frameworks or side chains have been constructed as catalysts for CO_2 transformation reaction, which include porous ionic polymers[22,38], hypercrosslinked polymers[39], and covalent organic frameworks[40]. Meanwhile, the research of heterogeneous catalysts that efficiently catalyze various CO_2 transformation reactions is still attractive and challenging.

Covalent organic framework(COF) is one of the outstanding porous polymers with ordered skeletons, high crystallinity, and permanent porosity. The monomers to construct COFs are multiple and can be functionalized smartly. Furthermore, COFs can be manufactured by elaborately manipulating the building blocks to obtain expected pore geometry, pore size, and ordered component arrangement. Two-dimensional(2D) COFs have rigid and regular one-dimensional(1D) channels, which is in favor of the mass transport during dynamic reactions and facilitates the enrichment of substrates[41,42]. The aforementioned features endow 2D COFs with intrinsic superiority to be platforms for heterogeneous catalysts. Actually, catalytic COFs with synergistic effects, where the catalytic sites are immobilized by post-synthesis process have been applied in numerous heterogeneous catalytic reactions[43—45]. The post-synthesis strategy is suitable to make small-molecule catalysts heterogeneous and upgrade the performance of COF-based catalysts[46]. We thence resort to reticular chemistry due to the controllability of building blocks and designability of diverse functional groups(or catalytically active sites) with atomic precision[47,48], and choose COFs as supports for catalysts to deal with the challenges of molecule phosphorus catalysts.

Herein, we utilize hydroxyl functionalized COFs as precursor to fabricate catalytic COFs with immobilized quaternary phosphonium salts to enhance the catalytic ability.

In the CO_2 reduction reaction, formamide and methylamine can be obtained *via* the reaction between CO_2, amines, and phenylsilane($PhSiH_3$) under gentle reaction conditions. The high yield of certain product is achieved by facilely adjusting reaction temperature. In the CO_2 fixation reaction, epoxide and aziridine with different substituent groups are efficiently transformed to cyclic carbonate and 5-aryl-2-oxazolidinone, respectively. Furthermore, the catalytic COFs are reusable as heterogeneous catalysts.

2 Experimental Section

2.1 Preparation of [PTPP]$_{x\%}$-TD-COFs

To a round bottom flask(50 mL), [OH]$_{50\%}$-TD-COF(28.7 mg), 3-bromopropyltriphenylphosphonium(46.4 mg, 0.10 mmol), K_2CO_3(30.0 mg, 0.22 mmol), and 5.00 mL of *N,N*-dimethylformamide(dried with molecular sieve) were added. The reactants were stirred at reflux for 36 h[42]. Then, the mixture was cooled down and centrifuged to obtain the solid. After washing with methanol and acetone, the solid product was collected and dried at 120 °C in a vacuum oven. The obtained black red solid was named as [PTPP]$_{50\%}$-TD-COF [yield: 72%, PTPP=3-bromopropyltriphenylphosphonium; TD=1,3,5-tri(4-amino-phenyl)benzene-1,4-diformylbenzene]. Other [PTPP]$_{x\%}$-TD-COFs(*X*=25 and 75, yield: 76% and 70%) were synthesized through an analogous method by corresponding [OH]$_{x\%}$-TD-COFs.

2.2 CO₂ Reduction Reaction to Prepare Formamide

[PTPP]$_{50\%}$-TD-COF(18.0 mg) was added in a two-neck flask(50 mL) that was equipped with a CO_2 balloon. Three vacuum-CO_2 refilling cycles were conducted to exhaust air in the reaction system. Then, amine(1.0 mmol), CH_3CN(2.00 mL), and $PhSiH_3$ (247 μL, 2.0 mmol) were added to the flask sequentially by syringe(solid amine at room temperature was dissolved into CH_3CN). The mixture was stirred at room temperature(RT) for 24 h. Then, ethyl acetate(10.0 mL) was injected to stop the reaction and excessive CO_2 was vented slowly. The liquid phase was collected through filtration, which was evaporated under reduced pressure after drying by anhydrous sodium sulfate. Finally, ^1H NMR test of the crude product in $CDCl_3$ was performed to confirm the conversion and yield.

2.3 CO₂ Reduction Reaction to Prepare Methylamine

[PTPP]$_{50\%}$-TD-COF(18.0 mg) was added in a two-neck flask (50 mL) that was equipped with a condenser pipe and a CO_2 balloon. Three vacuum-CO_2 refilling cycles were conducted to

exhaust air in the reaction system. The reactor was put into preheated oil bath(80 °C). Then, amine(1.0 mmol), CH_3CN(2.00 mL), and $PhSiH_3$(494 μL, 4.0 mmol) were injected into the flask successively and the mixture was stirred for 12 h. After the system was cooled down to 0 °C, ethyl acetate(10.0 mL) was injected to stop the reaction and excessive CO_2 was vented slowly. The liquid phase was collected through filtration, which was evaporated under reduced pressure after drying by anhydrous sodium sulfate. Finally, ^1H NMR test of the crude product in $CDCl_3$ was performed to confirm the conversion and yield.

2.4 Synthesis Method of Cyclic Carbonate

[PTPP]$_{50\%}$-TD-COF(15.0 mg) and epoxide(1.0 mmol) were added in a 10 mL(inner volume) stainless steel autoclave connected to a CO_2 cylinder. Three vacuum-CO_2 refilling cycles were conducted to exhaust air in the reaction system. After the CO_2 pressure was tuned to 2.0 MPa, the autoclave was put into the oil bath(100 °C) and reacted for 24 h. Then, the autoclave was cooled down to 0 °C and excessive CO_2 was discharged slowly. Dichloromethane(10.0 mL) was added and the mixture was filtered. The collected filtrate was evaporated under reduced pressure after drying by anhydrous sodium sulfate. Finally, ^1H NMR test of the crude product in $CDCl_3$ was performed to confirm the conversion and yield.

2.5 Synthesis Method of 5-Aryl-2-oxazolidinone

[PTPP]$_{50\%}$-TD-COF(10.0 mg) and aziridine(1.0 mmol) were added in a 10 mL(inner volume) stainless steel autoclave connected to a CO_2 cylinder. Three vacuum-CO_2 refilling cycles were conducted to exhaust air in the reaction system. After the CO_2 pressure was tuned to 3.0 MPa, the autoclave was put into the oil bath(80 °C) and stirred for 4—12 h. Then, the autoclave was cooled down to 0 °C and excessive CO_2 was discharged slowly. Dichloromethane(10.0 mL) was added and the mixture was filtered. The collected filtrate was evaporated under reduced pressure after drying by anhydrous sodium sulfate. Finally, ^1H NMR test of the crude product in $CDCl_3$ was performed to confirm the conversion and yield.

3 Results and Discussion

The 2D [OH]$_{X\%}$-TD-COFs(Scheme 1) with different amounts of hydroxyl group were synthesized under solvothermal reaction conditions by combining 1,3,5-tri(4-aminophenyl)benzene (TAPB), 2,5-dihydroxyterephthalaldehyde(DHTA), and 2,5-dimethoxyterephthalaldehyde(DMTA). Thereinto, the $X\%$ stands for the mole percentage of DHTA in dialdehyde mixture, which can be adjusted from 0 to 100%. In our previous
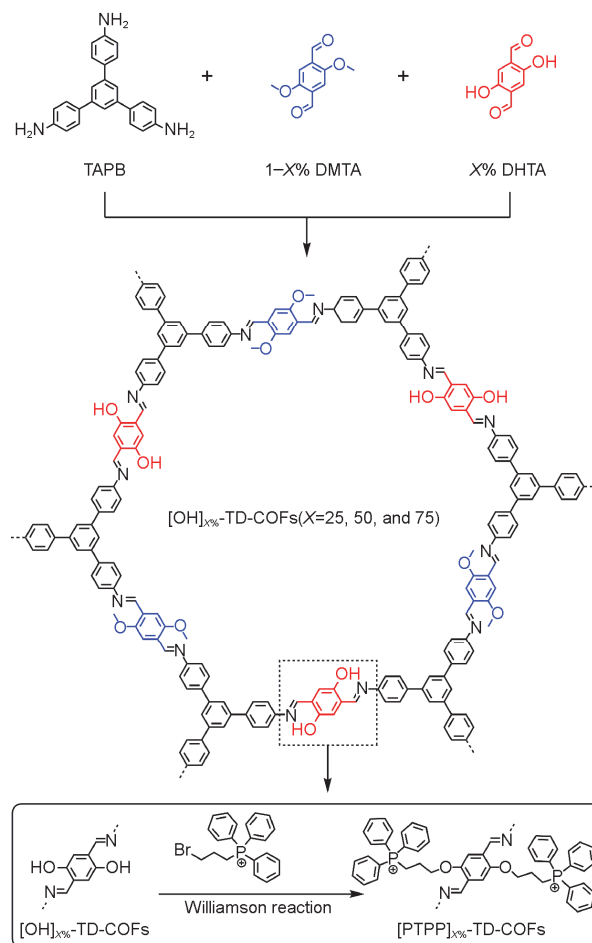
Scheme 1 Construction and functionalization of [OH]$_{X\%}$-TD-COFs

research, the porosity of [OH]$_{100\%}$-TD-COF is severely damaged after functionalization[49]. Therefore, the values of X selected in the research are 25, 50, and 75 to ensure the appropriate catalytic site density and high porosity of COFs after the post-synthesis modification. The quaternary phosphonium salt group was immobilized onto the channel wall of the COFs, [PTPP]$_{X\%}$-TD-COFs(X=25, 50, and 75), by Williamson reaction between —OH on [OH]$_{X\%}$-TD-COFs and PTPP. The element content of [PTPP]$_{X\%}$-TD-COFs is generally unanimous with the theoretically calculated value(Table S1, see the Electronic Supplementary Material of this paper). The concentration of anchored phosphonium is tuned accurately by adjusting the molar proportion of DHTA in the frameworks.

The crystallinity properties of COFs were tested by powder X-ray diffraction(PXRD)[Fig.1(A)]. The prominent peaks of [OH]$_{50\%}$-TD-COF appearing at 2θ=2.76°, 4.77°, 5.53°, 7.33°, 9.64°, and 25.18° are attributed to the crystal faces of (100), (110), (200), (210), (220), and (001), respectively. Lattice parameters of [OH]$_{50\%}$-TD-COF were obtained by Pawley refinements in Material Studio. The AA stacking model [Fig.1(C)] with $P2/m$ space group(a=7.41645 nm, b=7.54387 nm,
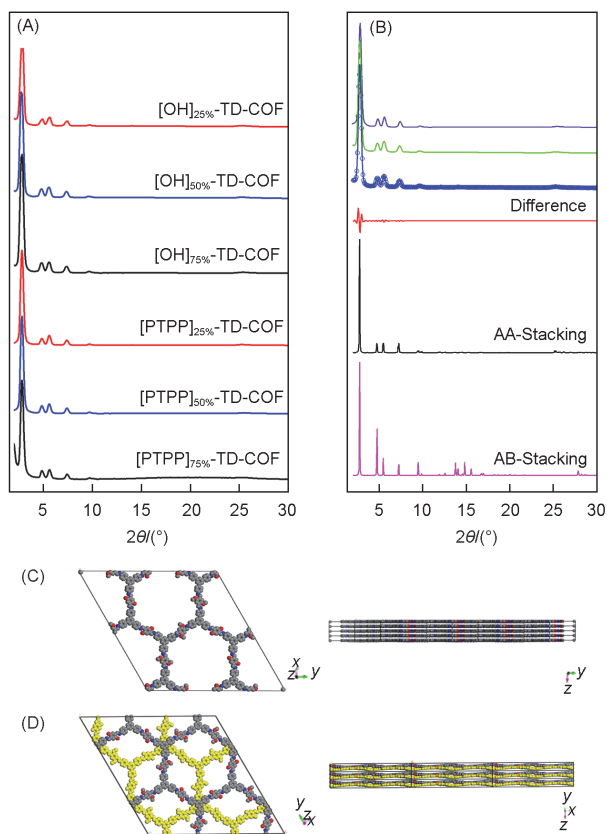
Fig.1 PXRD patterns of COFs(A), measured pattern(purple) of [PTPP]$_{50\%}$-TD-COF, measured(green) and refined(blue) patterns and their difference(red) for [OH]$_{50\%}$-TD-COF, simulated patterns of AA(black) and AB(magenta) stacking(B), and schematic diagram of AA(C) and AB(D) stacking models along *z*(left) and *y*(right) axes

c=0.35381 nm, $\alpha=\beta=90°$, and $\gamma=119.98°$) matches well with the experimental peak positions[Fig.1(B)]. In contrast, the AB stacking mode[Fig.1(D)] shows a distinguishable difference with the measured PXRD pattern. In addition, the patterns of COFs before and after functionalization do not exhibit obvious change, which is consistent with the previous report[49] and means that the ratio of DHTA/DMTA and PTPP has merely negligible effect on the ordered porous structures.

We conducted systematic measurements to confirm the successful fixation of PTPP in COFs. In Fourier transform infrared(FTIR) absorption spectra(Fig.S1, see the Electronic Supplementary Material of this paper), the stretching vibration peak of hydroxyl(3455 cm^{-1}) disappears after the functionalization process, which illustrates the exhaustion of hydroxyl in Williamson reaction. X-Ray photoelectron spectroscopy(XPS) measurement exhibits an overall outlook of the surface element compositions of the COFs(Fig.S2, see the Electronic Supplementary Material of this paper). The result indicates that [OH]$_{50\%}$-TD-COF contains 82.81% carbon, 7.00% nitrogen, and 10.19% oxygen(atomic fraction). In contrast, [PTPP]$_{50\%}$-TD-COF includes 74.39% carbon, 6.37% nitrogen,

15.68% oxygen, and 1.56% phosphorus. The P$_{2p}$ peak in XPS spectrum of [PTPP]$_{50\%}$-TD-COF suggests the successful post-synthesis functionalization. To further verify the presence of phosphorus, the solid-state ^{31}P NMR spectra were measured and the results also indicate the anticipative immobilization of PTPP on COFs. The ^{31}P signal of [PTPP]$_{50\%}$-TD-COF has about δ 8 shift to low field as compared with that of PTPP in CD$_3$OD, which is assumed to the varied environment effect on quandary phosphonium salt from CD$_3$OD to COFs[Fig.S3(A), see the Electronic Supplementary Material]. The solid-state ^{13}C NMR spectra of [PTPP]$_{X\%}$-TD-COF and [OH]$_{X\%}$-TD-COF do not show obvious distinction, which indicates the perfect maintenance of parent skeletons[Fig.S3(B), see the Electronic Supplementary Material of this paper]. The element mappings(Fig.S4, see the Electronic Supplementary Material of this paper) measured by scanning electron microscopy-energy dispersive X-ray spectroscopy(SEM–EDX) show that COF-based elements(C, N, and O) and functional elements (P and Br) are uniformly distributed in [PTPP]$_{50\%}$-TD-COF. Thermogravimetric analysis(TGA) results indicate that [PTPP]$_{X\%}$-TD-COFs cannot be obviously decomposed until the temperature increases to 400 °C(Fig.S5, see the Electronic Supplementary Material of this paper). These results demonstrate that the COF structure has enough thermal stability to support [PTPP]$_{X\%}$-TD-COFs as reusable catalysts at high reaction temperature. As for the chemical stability, it has been demonstrated by the well-maintained crystallinity after stirring in various common solvents at room temperature for a week(Fig.S6, see the Electronic Supplementary Material of this paper).

Nitrogen sorption isotherms were measured at 77 K to determine the porous properties of COFs, which possess type IV isotherms(Fig.2). For [OH]$_{X\%}$-TD-COFs, the Brunauer-Emmett-Teller specific surface areas proportionately decline along with the increased content of DHTA(Table S2, see the Electronic Supplementary Material). The different interactions of hydroxyl on DHTA and methoxy on DMTA in COF structure may account for the decreased surface area[41,50]. After the post-synthesis modification, the pore volumes and surface areas of [PTPP]$_{X\%}$-TD-COFs exhibit a disproportionate decrease with the increment of $X\%$, which is attributed to the space occupation of the grafted PTPP groups and their counterpart anions(Br$^-$). Meanwhile, the pore size tends to decrease slightly from 3.24 nm to 3.16—3.22 nm for [PTPP]$_{X\%}$-TD-COFs(Table S2). The minimal change of pore size is also observed in other post-synthesis functionalized COFs[41,44,45]. The abovementioned results demonstrate the success of developing catalytic COFs with varying active site contents and porosity, but retentive crystallinity *via* changing the molar percentage of DHTA in building blocks.

The successful combination between PTPP and COFs with

maintained features propels us to further verify the hypothesis that the catalytic activity of [PTPP]$_{X\%}$-TD-COFs will be enhanced as compared with [OH]$_{X\%}$-TD-COFs and PTPP. In the initial experiment, we chose N-methylaniline(**1a**) as a substrate in the CO_2 reduction reaction(Table 1). This reaction cannot proceed without PTPP, regardless of the presence or absence of [OH]$_{X\%}$-TD-COFs(Table 1, entries 1—4), which suggests that PTPP plays an indispensable role in the reaction. It also demonstrates that the product cannot be obtained without the participation of CO_2 either(Table 1, entry 14).

Notably, the catalytic performances exhibit different tendencies with the varied density of active sites on [PTPP]$_{X\%}$-TD-COFs(Table 1, entries 5—13). It is apparent and comprehensible that the catalyst possesses enhanced catalytic activity with the incremental PTPP immobilized on the channel wall at both the high and low reaction temperatures, in terms of substrate conversion. As compared with molecular catalysts(Table 1, entries 15 and 16), [PTPP]$_{X\%}$-TD-COFs(X=50 and 75) catalyze the CO_2 reduction reaction with a high conversion rate under mild conditions. The ordered and
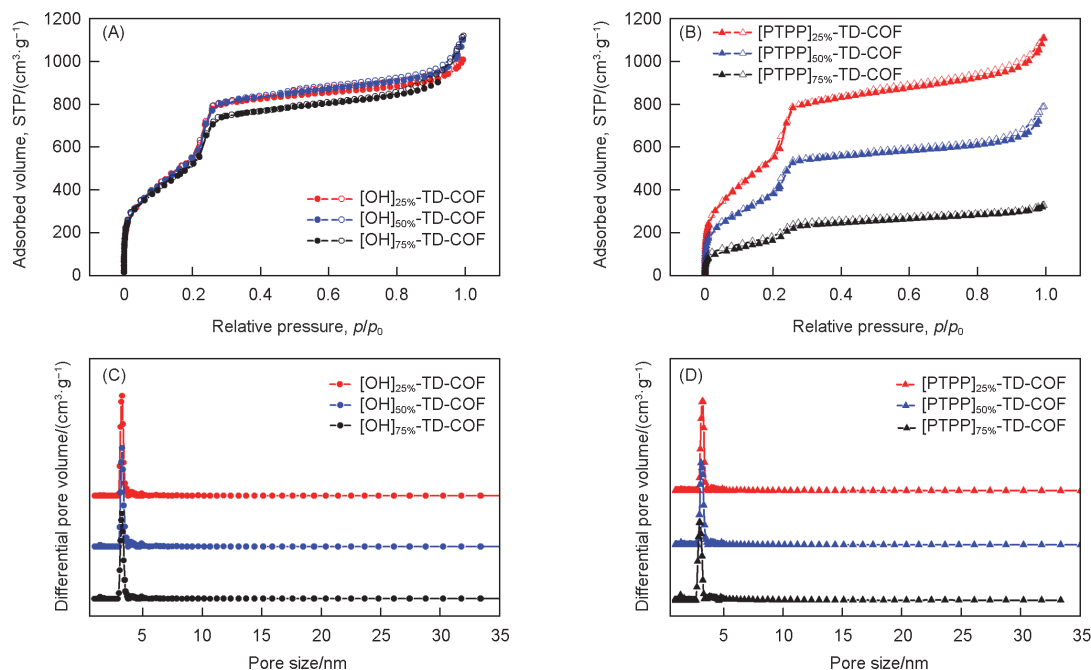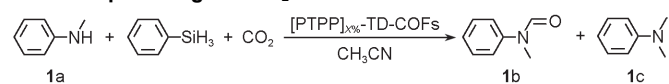

Fig.2 Nitrogen sorption isotherms(A, B) and pore size distributions(C, D) of [OH]$_{X\%}$-TD-COFs(A, C) and [PTPP]$_{X\%}$-TD-COFs(B, D)

Table 1 Optimizing the CO_2 reduction reaction condition^a

| Entry	Catalyst	T/°C	p_{CO_2}/MPa	Conv.^{b}(%)	Yield(%)	
				1a	**1b**	**1c**
1	None	60	0.1	0	0	0
2	[OH]$_{75\%}$-TD-COF	60	0.1	0	0	0
3	[OH]$_{50\%}$-TD-COF	60	0.1	0	0	0
4	[OH]$_{25\%}$-TD-COF	60	0.1	0	0	0
5	[PTPP]$_{75\%}$-TD-COF	60	0.1	99	55	45
6	[PTPP]$_{75\%}$-TD-COF	40	0.1	99	75	25
7	[PTPP]$_{75\%}$-TD-COF	R.T.	0.1	99	91	9
8	[PTPP]$_{50\%}$-TD-COF	60	0.1	99	44	56
9	[PTPP]$_{50\%}$-TD-COF	40	0.1	99	75	25
10	[PTPP]$_{50\%}$-TD-COF	R.T.	0.1	99	97	3
11	[PTPP]$_{25\%}$-TD-COF	60	0.1	85	83	2
12	[PTPP]$_{25\%}$-TD-COF	40	0.1	43	41	1
13	[PTPP]$_{25\%}$-TD-COF	R.T.	0.1	21	21	Trace
14^c	[PTPP]$_{50\%}$-TD-COF	60	0.0	0	0	0
15	PTPP	R.T.	0.1	5	5	Trace
16^d	Phosphorus Ylides	100	2.0	99	91	8

a. Reaction condition: N-methylaniline(1.0 mmol, 108 µL), phenylsilane(2.0 mmol, 247 µL), [PTPP]$_{X\%}$-TD-COFs[2.6%(molar ratio) based on PTPP catalytic sites relative to amine], and acetonitrile(2.00 mL), 24 h; *b* ^{1}H NMR measurement was used to determine the conversion and yield; *c* N$_2$ balloon; *d*. result in the reported literature[21].
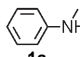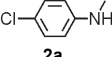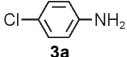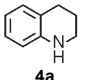
porous structures are conducive to reactant enrichment, substance transfer, and exposure of catalytic sites, which endow [PTPP]$_{x\%}$-TD-COFs with efficient catalytic performance. The selectivity between compounds **1**b and compound **1**c shows a different tendency when the reaction temperature changes. The yield of compound **1**b(formylation) increases with temperature declining, while the yield of compound **1**c(methylation) decreases in the reaction using [PTPP]$_{50\%}$-TD-COF as catalyst(Table 1, entries 8—10). This phenomenon has been reported by other analogous research and it has been supposed that the mechanisms of methylation and formylation are assigned to the thermodynamic and kinetic process, respectively[17,51,52]. The analogous situation happens to [PTPP]$_{75\%}$-TD-COF(Table 1, entries 5—7), but the variance of reaction selectivity is not as intense as [PTPP]$_{50\%}$-TD-COF. Nevertheless, the yields of compounds **1**b and **1**c with [PTPP]$_{25\%}$-TD-COF as catalyst show no dramatic change (Table 1, entries 11—13). We made a reasonable presumption for these results. High PTPP content with superior catalytic ability has poor discrimination for the disparity of energy-level in different reaction paths. This result signifies the distinction for thermodynamic and kinetic processes is weak with temperature alteration. While low content catalyst cannot catalyze the form of over-reduction product(methylamine) based on amine(with six-electron reduction) effectively, so a suitable amount of catalytic sites is required in the reaction. Among the three catalysts, [PTPP]$_{50\%}$-TD-COF possesses both high catalytic activity and temperature-dependent selectivity. From another perspective, excessive PTPP loaded on the channel wall will occupy the pore space, which has been illustrated by the significantly decreased porosity with the increasing content of PTPP. Superabundant PTPP retards the mass transport velocity in the channel and is unfavorable to the kinetic process. Considering the porosity, catalytic performance, selectivity, and economic principle, [PTPP]$_{50\%}$-TD-COF is our ultimate selection as the catalyst in the following experiments unless especial statement.

With the moderate content of PTPP anchored onto the COFs, we can obtain the specific product with high selectivity and yield by controlling the reaction temperature. As the catalyst, [PTPP]$_{50\%}$-TD-COF shows the best catalytic performance and makes formylation or methylation predominant at a certain temperature, respectively. Therefore, [PTPP]$_{50\%}$-TD-COF was selected to explore the substituent group tolerance and the scope of application(Table 2). In the formylation reaction of amine, diverse secondary amines are converted to formamides with a high yield and selectivity under mild conditions, indicating the wide applicability and high catalytic activity(Table 2, entries 1, 2, and 4). It's noteworthy that the electron-withdrawing substituent group almost does not diminish the catalytic performance, though the reaction is classified as electrophilic reaction in mechanism (Table 2, entry 2). [PTPP]$_{50\%}$-TD-COF also performs the formylation of primary amine with good selectivity and yield(Table 2, entry 3). The production of *N*-(4-chlorophenyl)-formamide(**3**b) suggests that the catalyst shows analogue catalytic behavior for both primary and secondary amines to afford monoformylation products in the formylation reaction. As for the stability and reusability of [PTPP]$_{50\%}$-TD-COF, we conducted cycling experiments with compound **1**a to verify the catalytic cycling performance. The catalyst was recycled and used again in a new reaction. In the second and third cycles, the yields of compound **1**b decrease to 53% and 22%, respectively. As compared with other reported catalysts for the formylation reaction that needs high temperature, high catalyst loading, or/and high CO_2 pressure[17,18,21,27,53],

Table 2 CO_2 reduction reaction with various amines(a) catalyzed by [PTPP]$_{50\%}$-TD-COF to produce *N*-formylated(b) and *N*-methylated products(c)^a
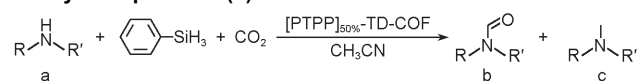
Entry	Substrate	For product b			For product c		
		Yield^b(%)	TON^c	TOF^d/h^{-1}	Yield^b(%)	TON^c	TOF^d/h^{-1}
1	**1a**	97(**1b**)	37	1.5	99(**1c**)	38	3.2
2	**2a**	93(**2b**)	36	1.5	91(**2c**)	35	2.9
3	**3a**	85(**3b**)	33	1.4	50(**3c**)^e	19	1.6
4	**4a**	99(**4b**)	38	1.6	89(**4c**)	34	2.8

a. *N*-Formylation condition: amine(1.0 mmol), phenylsilane(2.0 mmol, 247 μL), [PTPP]$_{50\%}$-TD-COF[18.0 mg, 2.6%(molar ratio) based on PTPP catalytic sites relative to amine], and acetonitrile(2.00 mL), room temperature, 24 h. *N*-Methylation condition: amine(1.0 mmol), phenylsilane(4.0 mmol, 494 μL), [PTPP]$_{50\%}$-TD-COF(18.0 mg, 2.6 mol%), and acetonitrile(2.00 mL), 80 °C, 12 h; *b* ^{1}H NMR measurement was used to determine the yield; *c* turnover number(TON)=mmol(product)/mmol(PTPP catalytic site); *d* turnover frequency(TOF)=mmol(product)/[mmol(PTPP catalytic site) ×(reaction time)]; *e* *N*,*N*-dimethylamine.

[PTPP]$_{50\%}$-TD-COF achieves heightened catalytic performance in catalyzing CO_2 reduction reaction with secondary amine and hydrogen silane to afford formamide under mild reaction conditions. Meanwhile, the catalytic performance of [PTPP]$_{50\%}$-TD-COF is comparable to those of reported COFs containing different functional groups(such as ionic liquid[44], imidazolium salt[54], and metal[55]) and other kinds of POPs[56,57] (Table S3, see the Electronic Supplementary Material of this paper).

In the methylation reaction, [PTPP]$_{50\%}$-TD-COF also exhibits excellent catalytic performance for secondary amine. Nevertheless, we obtained only *N,N*-dimethylamine product (**3**c) in the methylation of primary amine. The reason is assumed that the produced monomethyl secondary amine proceeds further methylation more quickly than formylation. Thus, the *N,N*-dimethylamine is the ultimate product of methylation of primary amine[52]. Furthermore, the reaction time of methylation of amine can be halved due to the improved reaction rate with the increased reaction temperature.

Further investigations were performed in order to reveal the role that [PTPP]$_{50\%}$-TD-COF played during the catalytic reaction. First, ^{1}H NMR analysis was performed to explore the impact of [PTPP]$_{50\%}$-TD-COF on PhSiH$_3$. We added [PTPP]$_{50\%}$-TD-COF(1.6%, molar fraction) and PhSiH$_3$(2.0 mmol) to acetonitrile-d$_3$(2.00 mL) and stirred the mixture for 10 h under N$_2$. The ^{1}H NMR spectra show that the signal peak of Si—H in the mixture possesses a slight shift(δ 4.19) as compared with that(δ 4.21) of pure PhSiH$_3$(Fig.S7, see the Electronic Supplementary Material of this paper), which represents the activation of Si—H by [PTPP]$_{50\%}$-TD-COF[44]. The possible reason is the interaction between phosphorus cation and electronegative hydrogen atom on PhSiH$_3$. Second, we proved the effect of [PTPP]$_{50\%}$-TD-COF on facilitating the CO_2 reduction reaction. In two control experiments, [PTPP]$_{50\%}$-TD-COF and [OH]$_{50\%}$-TD-COF were utilized as catalysts, respectively. The mixture of acetonitrile-d$_3$, CO_2(0.1 MPa),

PhSiH$_3$, and COF was stirred at room temperature for 6 h. The ^{1}H NMR spectroscopy measurement was utilized to analyze the products(Fig.S8, see the Electronic Supplementary Material of this paper). A new signal peak(δ 8.17) assigned to the hypervalent silicon species appears in ^{1}H NMR spectrum of the reactant catalyzed by [PTPP]$_{50\%}$-TD-COF[58,59], which demonstrates the catalytic effect of [PTPP]$_{50\%}$-TD-COF straightway.

Based on the result and analysis of the abovementioned characterizations, a possible reaction mechanism was proposed according to the previous reports(Scheme 2)[60—62]. The phosphonium first interacts with electronegative oxygen of CO_2[63,64], as well as the hydrogen of PhSiH$_3$. The existence of three phenyls in PTPP that have large steric hindrance prevents the combination of activated species with counter ions. Thus, the activated Si—H and CO_2 have enough possibility to interact with each other. The oxygen on CO_2 with an increased electron cloud density attacks the silicon atom of PhSiH$_3$ with a diminished electron cloud density to form the hypervalent silicon species(**A**)[65]. Afterwards, the active hydrogen with a couple of electrons is transformed from PhSiH$_3$ to the positive carbon atom of CO_2 to generate phenylsilyl formate(**B**). **B** would conduct a further catalytic cycle to obtain the C^0 silyl acetal(**D**) when the reaction is performed at a high temperature. Then, the oxygen atoms on **D** are substituted by the nitrogen atom of amine to afford the C^0 aminal(**E**). **E** will conduct another catalytic cycle to form the methyl-product (methylamine, **F**)[52]. Nonetheless, when the reaction is carried out at room temperature, almost all **B** will suffer from the nucleophilic substitution by amine to yield formamide(**C**) instead of the generation of **D**, **E**, and finally **F**. Presumably, in contrast to the generation of **C**, the process from **B** to **D** is thermodynamically favorable, which proceeds smoothly when there is sufficient activation energy. Here, the temperature is the only representation of activation energy level when using a certain catalyst. Single product(**C** or **F**) can be produced selectively by adjusting the reaction temperature.
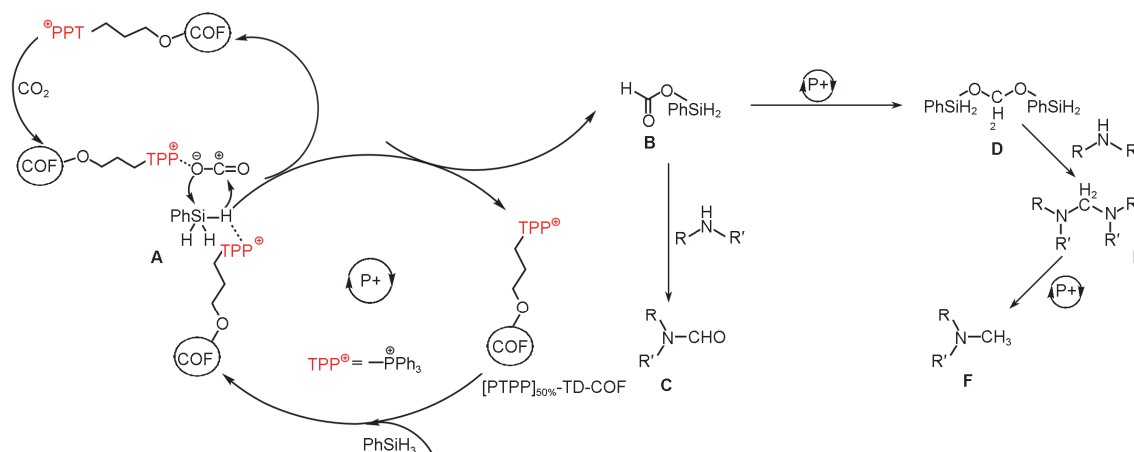
Scheme 2 Supposed mechanism of CO_2 reduction reaction with amine and phenylsilane catalyzed by [PTPP]$_{50\%}$-TD-COF
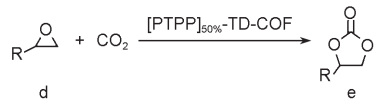
Motivated by the improved catalytic ability of [PTPP]$_{50\%}$-TD-COF in CO_2 reduction reaction, we further explored the catalytic performance of [PTPP]$_{50\%}$-TD-COF in other kinds of CO_2 transformation reactions. It has been reported that quaternary phosphonium salts are immobilized onto various supports, such as silica[66], chitosan[67], and porous polymers[39], as catalysts in the cycloaddition reaction between CO_2 and epoxide. However, the performance is not very ideal due to the demanding reaction condition and inadequate conversion of aromatic epoxide. The distinctive features of COFs, such as uniform pore size, ordered structure, and designability and controllability of active sites endow COFs with inherent advantages as supports for molecular catalysts. Correspondingly, we continued to explore the application of [PTPP]$_{50\%}$-TD-COF as catalyst in the CO_2 conversion reaction. According to the reported work, aryl epoxides are harder to accomplish the cycloaddition reaction than some alkyl substrates at the same reaction condition[68]. Therefore, we chose 2-(phenoxymethyl)oxirane(**1d**) as the substrate in the benchmark reaction to ensure that the optimized reaction condition is suitable for all epoxides. The results(Table 3, entries 1—3) exhibit that a high enough temperature(140 °C) ensures the complete conversion of compound **1d**. In order to gentle the reaction condition without sacrificing the conversion rate, we tried to increase the pressure of CO_2 to compensate for the temperature drop(Table 3, entries 4—6). The reaction condition in Table 3, entry 5 is confirmed as the optimum one for the cycloaddition reaction. Furthermore, diverse epoxides were utilized in the CO_2 cycloaddition reaction. The results show that [PTPP]$_{50\%}$-TD-COF possesses excellent functional group tolerance(Table 3, entries 7—9).
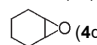
The reaction between CO_2 and epoxide is assigned to a kind of electrophilic cycloaddition reaction[23]. Wherein, the electrophilic groups like $ClCH_2$— on epoxide favor the reaction by sharing the negative charge with the oxygen atom.

The attack of the positive charge group(phosphorus cation) to the oxygen of epoxide is always the first step in the cycloaddition reaction. Almost simultaneously, active CO_2 reacts with the positive part of the three-membered loop in epoxide to open the loop(Scheme S1, see the Electronic Supplementary Material of this paper). Subsequently, the cyclic carbonate with a five-membered ring is formed by a loop-closing reaction.

In addition, the ordered channel structure with sensitivity for the steric hindrance of isomer products endows [PTPP]$_{50\%}$-TD-COF with an ability to impede the generation of products with large steric inhibition, which means the catalyst should have significant advantages in producing the specific isomer selectivity. We chose the reaction between CO_2 and aziridine with different substituent groups to demonstrate this hypothesis(Table 4). The reaction will produce a couple of constitutional isomers, 5-aryl-2-oxazolidinone and 6-aryl-2-oxazolidinone, because of the different bond-breaking positions in the asymmetric structure of aziridine. Generally, the way to obtain the less steric hindrance product, 5-aryl-2-oxazolidinone(g), will undergo an intermediate state with positive charge carbon adjacent to the group R_1(Scheme S1)[24,25,63]. The group R_1 with electron donating effect will greatly stabilize the intermediate and facilitate the reaction to produce 5-aryl-2-oxazolidinone(Table 4, entries 1—5). Otherwise, it is difficult to perform the reaction(Table 4, entries 6—9). When the quaternary phosphonium salts are immobilized on COFs, [PTPP]$_{50\%}$-TD-COF inherits the ordered pore structure of original COFs and possesses superior regioselectivity as compared with homogeneous catalysts. Various aziridines with phenyl as R_1 and different N-alkyl groups(R_2) are transformed into 5-aryl-2-oxazolidinones efficiently with [PTPP]$_{50\%}$-TD-COF as catalyst(Table 4, entries 3—5).
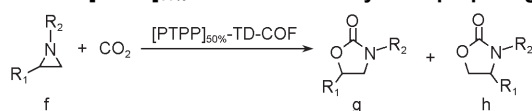
Table 3 Cycloaddition reaction between CO_2 and epoxide catalyzed by [PTPP]$_{50\%}$-TD-COF [a]

Entry	Substrate(R—)	T/°C	p_{CO_2}/MPa	Yield[b](%)	TON[c]	TOF[d]/h^{-1}
1	PhOCH$_2$(**1d**)	80	0.1	Trace(**1e**)	0	0.0
2	PhOCH$_2$(**1d**)	120	0.1	94(**1e**)	47	3.9
3	PhOCH$_2$(**1d**)	140	0.1	99(**1e**)	49	4.1
4	PhOCH$_2$(**1d**)	120	2.0	99(**1e**)	49	4.1
5	PhOCH$_2$(**1d**)	100	2.0	99(**1e**)	49	4.1
6	PhOCH$_2$(**1d**)	80	2.0	7(**1e**)	4	0.3
7	Ph(**2d**)	100	2.0	99(**2e**)	49	4.1
8	ClCH$_2$(**3d**)	100	1.0	99(**3e**)	49	4.1
9[e]	(**4d**)	100	2.0	85(**4e**)	43	1.8

a. Reaction condition: epoxide(1.0 mmol), [PTPP]$_{50\%}$-TD-COF[15.0 mg, 2.0%(molar fraction) based on PTPP catalytic sites relative to epoxide], 12 h; *b*. ^{1}H NMR measurement was used to determine the yield; *c*. TON=mmol(product)/mmol(PTPP catalytic site); *d*. TOF=mmol(product)/[mmol(PTPP catalytic site)× (reaction time)]; *e*. reaction time was 24 h.

Table 4 [PTPP]$_{50\%}$-TD-COF as catalyst for preparing 5-aryl-2-oxazolidinone with aziridine and CO_2^{a}

Entry	Substrate(R_1, R_2)	p_{CO_2}/MPa	T/h	Conv.(%) f	Yield^b(%)		TON^c	TOF^d/h^{-1}
					g	h	g	g
1	Ph, Et(**1f**)	5	12	99	97(**1g**)	3	75	6.3
2	Ph, Et(**1f**)	3	3	75	75(**1g**)	Trace	58	19.3
3	Ph, Et(**1f**)	3	4	99	99(**1g**)	Trace	76	19.0
4	Ph, H(**2f**)	3	4	99	99(**2g**)	Trace	76	19.0
5	Ph, n-Pr(**3f**)	3	4	99	99(**3g**)	Trace	76	19.0
6	p-Cl-Ph, Et(**4f**)	3	4	22	21(**4g**)	Trace	16	4.0
7	p-Cl-Ph, Et(**4f**)	3	8	70	69(**4g**)	Trace	53	6.6
8	p-Cl-Ph, Et(**4f**)	3	12	99	99(**4g**)	Trace	76	6.3
9	p-Cl-Ph, n-Pr(**5f**)	3	12	78	78(**5g**)	Trace	60	5.0

a. Reaction condition: aziridine(1.0 mmol), [PTPP]$_{50\%}$-TD-COF[10.0 mg, 1.3%(molar fraction) based on PTPP catalytic sites relative to aziridine], reaction temperature 80 °C; *b*. ^{1}H NMR measurement was used to determine the conversion and yield; *c*. TON=mmol(product)/mmol(PTPP catalytic site); *d*. TOF=mmol(product)/[mmol(PTPP catalytic site) ×(reaction time)].

4 Conclusions

In summary, by post-synthesis pore engineering strategy, we successfully immobilized the quaternary phosphonium salt catalytic sites onto COFs. With the controllable density of catalyst and perfect maintaining of COF features, the catalytic [PTPP]$_{50\%}$-TD-COF catalyzes the CO_2 reduction reaction with amine and phenylsilane under mild reaction conditions with high efficiency and selectivity. Meanwhile, we demonstrated that the synergistic effect by combining COFs and homogeneous catalysts improves the catalytic performance. We further applied this heterogeneous catalyst to perform the CO_2 fixation reactions with epoxide and aziridine to afford cyclic carbonates and 5-aryl-2-oxazolidinones, respectively. [PTPP]$_{50\%}$-TD-COF possesses enhanced catalytic performance and applicability for CO_2 transformations owing to the high stability, crystallinity, and porosity. Undoubtedly, it is a new exploration in COF functionalization by post-synthesis strategy, and demonstrates again the superiority and universality of COFs as supports for molecular catalysts.

Electronic Supplementary Material

Supplementary material is available in the online version of this article at http://dx.doi.org/10.1007/s40242-022-1495-1.

Conflicts of Interest

The authors declare no conflicts of interest.

References

[1] Lashof D. A., Ahuja D. R., *Nature*, **1990**, *344*, 529
[2] Matter J. M., Stute M., Snæbjörnsdottir S. Ó., Oelkers E. H., Gislason S. R., Aradottir E. S., Sigfusson B., Gunnarsson I., Sigurdardottir H., Gunnlaugsson E., Axelsson G., Alfredsson H. A., Wolff-Boenisch D., Mesfin K., de la Reguera Taya D. F., Hall J., Dideriksen K., Broecker W. S., *Science*, **2016**, *352*, 1312
[3] Kirchner B., Intemann B., *Nat. Chem.*, **2016**, *8*, 401
[4] Allen M. R., Stocker T. F., *Nat, Clim. Change*, **2014**, *4*, 23
[5] Keith D. W., *Science*, **2009**, *325*, 1654
[6] Arneth A., Sitch S., Pongratz J., Stocker B. D., Ciais P., Poulter B., Bayer A. D., Bondeau A., Calle L., Chini L. P., Gasser T., Fader M., Friedlingstein P., Kato E., Li W., Lindeskog M., Nabel J. E. M. S., Pugh T. A. M., Robertson E., Viovy N., Yue C., Zaehle S., *Nat. Geosci.*, **2017**, *10*, 79
[7] Sakakura T., Choi J.-C., Yasuda H., *Chem. Rev.*, **2007**, *107*, 2365
[8] Yu B., He L.-N., *ChemSusChem*, **2015**, *8*, 52
[9] Liu Q., Wu L., Jackstell R., Beller M., *Nat. Commun.*, **2015**, *6*, 5933
[10] Yang Z.-Z., He L.-N., Gao J., Liu A.-H., Yu B., *Energ. Environ. Sci.*, **2012**, *5*, 6602
[11] Li K., Peng B., Peng T., *ACS Catal.*, **2016**, *6*, 7485
[12] Aresta M., Dibenedetto A., Angelini A., *Chem. Rev.*, **2014**, *114*, 1709
[13] Wang W. H., Himeda Y., Muckerman J. T., Manbeck G. F., Fujita E., *Chem. Rev.*, **2015**, *115*, 12936
[14] Wang W., Wang S., Ma X., Gong J., *Chem. Soc. Rev.*, **2011**, *40*, 3703
[15] Chueh W. C., Falter C., Abbott M., Scipio D., Furler P., Haile S. M., Steinfeld A., *Science*, **2010**, *330*, 1797
[16] Lim C. H., Holder A. M., Hynes J. T., Musgrave C. B., *J. Phys. Chem. Lett.*, **2015**, *6*, 5078
[17] Fang C., Lu C., Liu M., Zhu Y., Fu Y., Lin B.-L., *ACS Catal.*, **2016**, *6*, 7876
[18] Hao L., Zhao Y., Yu B., Yang Z., Zhang H., Han B., Gao X., Liu Z., *ACS Catal.*, **2015**, *5*, 4989
[19] Li Y., Cui X., Dong K., Junge K., Beller M., *ACS Catal.*, **2017**, *7*, 1077
[20] Lian Z., Nielsen D. U., Lindhardt A. T., Daasbjerg K., Skrydstrup T., *Nat. Commun.*, **2016**, *7*, 13782
[21] Zhou H., Wang G.-X., Zhang W.-Z., Lu X.-B., *ACS Catal.*, **2015**, *5*, 6773
[22] Wang W., Wang Y., Li C., Yan L., Jiang M., Ding Y., *ACS Sustainable Chem. Eng.*, **2017**, *5*, 4523
[23] Li P., Cao Z., *Organometallics*, **2018**, *37*, 406
[24] Yang Z.-Z., He L.-N., Peng S.-Y., Liu A.-H., *Green Chem.*, **2010**, *12*, 1850
[25] Watile R. A., Bagal D. B., Deshmukh K. M., Dhake K. P., Bhanage B. M., *J. Mol. Catal. A-Chem.*, **2011**, *351*, 196
[26] Jia J., Qian C., Dong Y., Li Y. F., Wang H., Ghoussoub M., Butler K. T., Walsh A., Ozin G. A., *Chem. Soc. Rev.*, **2017**, *46*, 4631
[27] Chong C. C., Kinjo R., *Angew. Chem. Int. Ed.*, **2015**, *54*, 12116
[28] Zhang Z., Fan F., Xing H., Yang Q., Bao Z., Ren Q., *ACS Sustainable Chem. Eng.*, **2017**, *5*, 2841
[29] Liang J., Xie Y. Q., Wu Q., Wang X. Y., Liu T. T., Li H. F., Huang Y. B., Cao R., *Inorg. Chem.*, **2018**, *57*, 2584
[30] Zulfiqar S., Sarwar M. I., Mecerreyes D., *Polym. Chem.*, **2015**, *6*, 6435
[31] Bayne J. M., Stephan D. W., *Chem. Soc. Rev.*, **2016**, *45*, 765
[32] Hill C. L., Prosser-McCartha C. M., *Coordin. Chem. Rev.*, **1995**, *143*, 407

[33] Prier C. K., Rankic D. A., MacMillan D. W. C., *Chem. Rev.*, **2013**, *113*, 5322

[34] Sun X.-L., Tang Y., *Accounts Chem. Res.*, **2008**, *41*, 937

[35] Li A.-H., Dai L.-X., Aggarwal V. K., *Chem. Rev.*, **1997**, *97*, 2341

[36] Matthews C. N., Driscoll J. S., Birum G. H., *Chem. Commun.(London)*, **1966**, 736

[37] Diercks C. S., Liu Y., Cordova K. E., Yaghi O. M., *Nat. Mater.*, **2018**, *17*, 301

[38] Hu K., Tang Y., Cui J., Gong Q., Hu C., Wang S., Dong K., Meng X., Sun Q., Xiao F.-S., *Chem. Commun.*, **2019**, *55*, 9180

[39] Wang J., Yang J. G. W., Yi G., Zhang Y., *Chem. Commun.*, **2015**, *51*, 15708

[40] Sun Q., Aguila B., Perman J., Nguyen N., Ma S., *J. Am. Chem. Soc.*, **2016**, *138*, 15790

[41] Xu H., Gao J., Jiang D., *Nat. Chem.*, **2015**, *7*, 905

[42] Fang Q., Gu S., Zheng J., Zhuang Z., Qiu S., Yan Y., *Angew. Chem., Int. Ed.*, **2014**, *53*, 2878

[43] Huang N., Wang P., Jiang D., *Nat. Rev. Mater.*, **2016**, *1*, 16068

[44] Dong B., Wang L., Zhao S., Rile G., Song X., Wang Y., Gao Y., *Chem. Commun.*, **2016**, *52*, 7082

[45] Huang N., Krishna R., Jiang D., *J. Am. Chem. Soc.*, **2015**, *137*, 7079

[46] Li Q., Li Z., *Polym. Chem.*, **2015**, *6*, 6770

[47] Diercks C. S., Yaghi O. M., *Science*, **2017**, *355*, eaal1585

[48] Ding S. Y., Wang W., *Chem. Soc. Rev.*, **2013**, *42*, 548

[49] Mu Z.-J., Ding X., Chen Z.-Y., Han B.-H., *ACS Appl. Mater. Interfaces*, **2018**, *10*, 41350

[50] Kandambeth S., Venkatesh V., Shinde D. B., Kumari S., Halder A., Verma S., Banerjee R., *Nat. Commun.*, **2015**, *6*, 6786

[51] Liu X.-F., Ma R., Qiao C., Cao H., He L.-N., *Chem.-Eur. J.*, **2016**, *22*, 16489

[52] Liu X.-F., Li X.-Y., Qiao C., Fu H.-C., He L.-N., *Angew. Chem., Int. Ed.*, **2017**, *56*, 7425

[53] Nguyen T. V., Yoo W. J., Kobayashi S., *Angew. Chem., Int. Ed.*, **2015**, *54*, 9209

[54] Qiu J., Zhao Y., Li Z., Wang H., Shi Y., Wang J., *ChemSusChem*, **2019**, *12*, 2421

[55] Cao Q., Zhang L.-L., Zhou C., He J.-H., Marcomini A., Lu J.-M., *Appl. Catal., B*, **2021**, *294*, 120238

[56] Lv H., Wang W., Li F., *Chem.-Eur. J.*, **2018**, *24*, 16588

[57] Luo R., Chen Y., He Q., Lin X., Xu Q., He X., Zhang W., Zhou X., Ji H., *ChemSusChem*, **2017**, *10*, 1526

[58] Revunova K., Nikonov G. I., *Chem.-Eur. J.*, **2014**, *20*, 839

[59] Xie W., Zhao M., Cui C., *Organometallics*, **2013**, *32*, 7440

[60] Hounjet L. J., Caputo C. B., Stephan D. W., *Angew. Chem., Int. Ed.*, **2012**, *51*, 4714

[61] Stephan D. W., Erker G., *Angew. Chem. Int. Ed.*, **2010**, *49*, 46

[62] Sajid M., Kehr G., Wiegand T., Eckert H., Schwickert C., Pöttgen R., Cardenas A. J. P., Warren T. H., Fröhlich R., Daniliuc C. G., Erker G., *J. Am. Chem. Soc.*, **2013**, *135*, 8882

[63] Song Q.-W., Zhou Z.-H., He L.-N., *Green Chem.*, **2017**, *19*, 3707

[64] Leitner W., *Coordin. Chem. Rev.*, **1996**, *153*, 257

[65] Liu X.-F., Qiao C., Li X.-Y., He L.-N., *Green Chem.*, **2017**, *19*, 1726

[66] Steinbauer J., Longwitz L., Frank M., Epping J., Kragl U., Werner T., *Green Chem.*, **2017**, *19*, 4435

[67] Chen J.-X., Jin B., Dai W.-L., Deng S.-L., Cao L.-R., Cao Z-J., Luo S.-L., Luo X.-B., Tu X.-M., Au C.-T., *Appl. Catal. A*, **2014**, *484*, 26

[68] Liu S., Suematsu N., Maruoka K., Shirakawa S., *Green Chem.*, **2016**, *18*, 4611